

[Supplementary Information for *Nanoscale* manuscript NR-ART-02-2019-001453]

Nanoscale toughening of ultrathin graphene oxide-polymer composites: mechanochemical insights into hydrogen-bonding/van der Waals interactions, polymer chain alignment, and steric parameters

Xu Zhang,^a Hoang Nguyen,^a Matthew Daly,^{b, #} SonBinh T. Nguyen,^{*c} Horacio D. Espinosa^{*a, b}

^aTheoretical and Applied Mechanics Program, Northwestern University, 2145 Sheridan Rd., Evanston, IL 60208, USA.

^bDepartment of Mechanical Engineering, Northwestern University, 2145 Sheridan Rd., Evanston, IL 60208, USA.

^cDepartment of Chemistry, Northwestern University, 2145 Sheridan Rd., Evanston, IL 60208, USA

*espinosa@northwestern.edu; stn@northwestern.edu

[^]These authors contributed equally to this work

[#]Present address: Department of Civil and Materials Engineering, University of Illinois at Chicago, Chicago, IL 60607, USA

Table of Contents

S1. Melt-state statistics of polymers	S1
S2. Critical energy release rate of the GO-polymer system	S2
S3. Rate-dependence of crack-opening simulations and the data for all polymers	S2
S4. Single-chain pull-off simulations for all polymers	S5
S5. Analysis of the cooperative behavior of HBs	S6
S6. Cost of computational resource	S6
S7. References	S7

S1. Melt-state statistics of polymers

To characterize the conformation of the polymer chains, we monitor the mean-square end-to-end distance ($\langle R^2 \rangle$) of the polymer chains, which scales differently with the number of repeating units in different environments,^{S1} e.g., good solvents, poor solvents, melt-states, etc. The mean-square end-to-end distance $\langle R^2 \rangle$ for a polymer in the melt state can be calculated from the ideal-chain approximation:

$$\langle R^2 \rangle \cong C_{\infty} n l^2 \quad (\text{S1})$$

where C_{∞} is Flory's characteristic ratio, n is the number of backbone bonds, and l is the backbone bond length.^{S1} The value n is 269 for PEG and 267 for all other polymers investigated herein. We use C_{∞} values that were reported elsewhere,^{S1, S2} and l is assumed to be 1.54 Å for all polymers. After attaining the target $\langle R^2 \rangle$, we calculated the root-mean-square end-to-end distance $R_0 = \sqrt{\langle R^2 \rangle}$ for each polymer. With the self-avoiding random-walk algorithm method, we generated six atactic polymer chains that have the average end-to-end distance R_a close to R_0 . Table S1 shows the corresponding data for each polymer.

Table S1. Conformational parameters, targeted end-to-end distance, and parameters used in simulations for all polymers.

Polymer	C_{∞} (Å)	$\langle R^2 \rangle$ (Å ²)	R_0 (Å)	R_a (Å)
PAA ^a	8.1 ^{S2}	5129.06	71.62	69.34 ± 2.18
PMA	8.1 ^{S2}	5129.06	71.62	72.80 ± 3.95
PBA ^b	9.3 ^{S2}	5888.92	76.74	73.82 ± 7.75
PVA ^c	7.6 ^{S2}	4812.45	69.37	70.20 ± 3.65
PEG	6.7 ^{S1}	4274.33	65.38	66.31 ± 2.21

^aBased on data for poly(methylacrylate). ^bBased on data for poly(ethylacrylate). ^cBased on data for poly(vinyl chloride).

S2. Critical energy release rate of the GO-polymer system

The fracture toughness of fiber-reinforced composites is characterized by a fracture resistance curve (R-curve), which shows the energy required to propagate a crack by an infinitesimal amount at a given crack length.^{S3} As an analogy to the fiber-reinforced composites, the GO-polymer systems can also be characterized by a fracture resistance curve, as shown in Fig. S1a. When a crack initiates on GO (Fig. S1b), the fracture resistance is equal to the intrinsic toughness of GO, namely, G_0 , as shown in Fig. S1a. Then, the polymer chains start to bridge the crack. As the crack propagates, more polymer chains bridge the crack (Fig. S1c), causing an increase of the fracture resistance (Fig. S1a). At a crack extension L_0 , the fracture resistance reaches G_0+G_f , where G_f is the energy release rate calculated from the crack-opening simulations (Fig. 4b). At this crack extension, the polymer chain that first bridges the crack is just pulled-off completely (Fig. S1d). If the conformations of polymers in front the crack tip (corresponding to the right of the crack tip in Fig. S1) are similar to those behind the crack tip, a crack extension after L_0 will lead to the same crack bridging scenario as Fig. S1d, therefore providing the same fracture resistance. The crack-opening simulations show non-negligible variances of G_f , and the fracture resistance, as a result, should fluctuate around the average value.

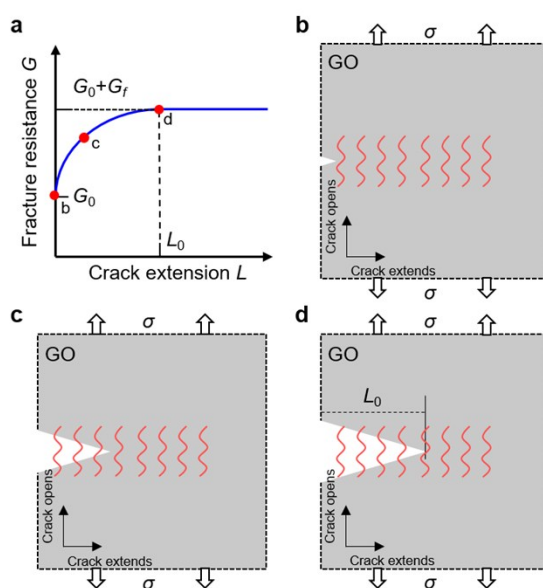


Fig. S1. Critical energy release rate with polymer crack-bridging. (a) Fracture-resistance curve for the GO-polymer systems. (b)-(d) Snapshots of the crack-bridging with the corresponding fracture resistance marked in (a).

S3. Rate-dependence of crack-opening simulations and the data for all polymers

To test the rate-dependence of the crack-opening simulations for both the hydrogen-bonding and van der Waals interactions, we selected two GO-polymer systems (GO-PAA and GO-PBA) and three strain rates ($10^8/s$, $10^9/s$, and $10^{10}/s$) that were selected to cover a broad enough range

without incurring excessive computation cost. For each GO-polymer system, the same initial polymer configuration was used for all the strain rates. Not surprisingly, the crack-opening simulation of the vdW-interacting GO-PBA system (Fig. S2b) is less sensitive to the variation in strain rate in comparison to that for the GO-PAA system (Fig. S2a). Nevertheless, the average T_{2D} values for both systems appear to reach fixed values as the strain rate was decreased to $10^9/s$, justifying our selection of this strain rate in the simulations.

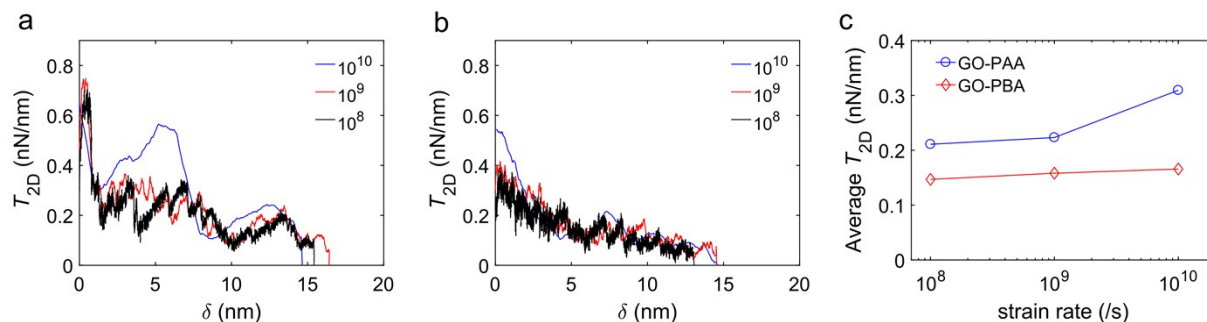


Fig. S2. Rate-dependent behaviors of the crack-opening simulations for representative hydrogen-bonding and vdW-interaction GO-polymer systems. (a) T_{2D} - δ curves for a GO-PAA system at three strain rates. (b) T_{2D} - δ curves for a GO-PBA system at three strain rates. (c) Average T_{2D} values taken from the data in (a) and (b) as a function of the strain rate.

Representative 2D traction (T_{2D})–crack-opening (δ) curves for all GO-polymer systems are shown in Fig. S3.

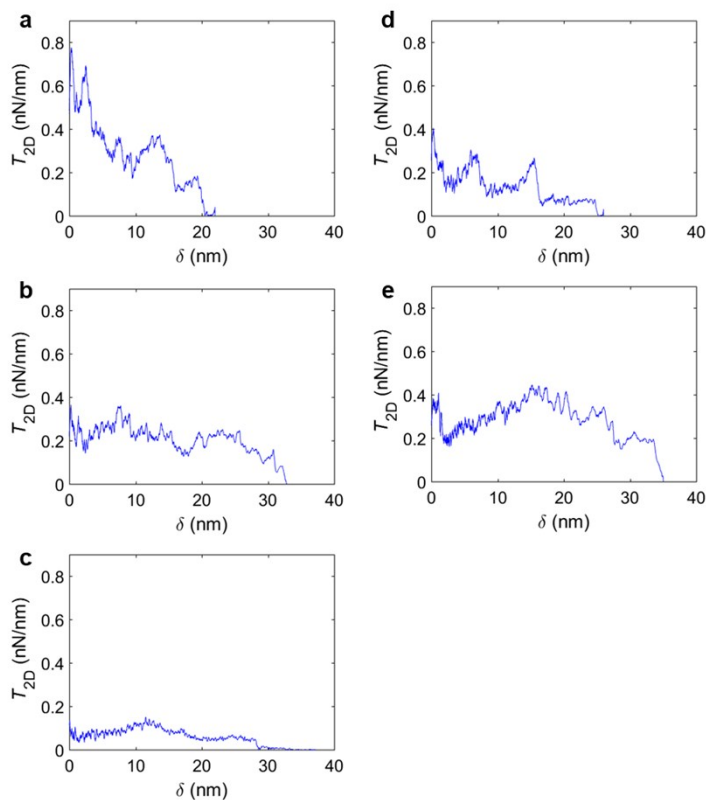


Fig. S3. T_{2D} - δ curves for (a) GO-PAA, (b) GO-PVA, (c) GO-PEG, (d) GO-PMA, and (e) GO-PBA systems.

The G_f and the fracture toughness enhancements of all polymers are shown in Table S2.

Table S2. G_f measurement of all polymers.

System	G_f (nJ/m) from six MD simulations						Random polymer chains G_f (nJ/m)	Toughness enhancement G_f/G_0^b (%)	Aligned polymer chains G_f (nJ/m)	Toughness enhancement G_f/G_0^b (%)
GO (G_0)	4						-	N/A	-	N/A
GO-PAA	6.39	11.64	4.56	4.88	12.16	3.76	7.23 ± 3.72	180	12.41	310
GO-PMA	2.25	3.53	2.22	4.32	3.66	7.04	3.84 ± 1.77	96	6.98	175
GO-PBA	6.20	9.94	6.93	1.50	1.89	5.88	5.39 ± 3.21	135	9.71	243
GO-PVA	1.66	6.73	3.32	5.19	4.92	2.21	4.01 ± 1.94	100	8.54	214
GO-PEG	2.11	2.41	1.58	1.50	1.56	1.26	1.74 ± 0.43	40	5.03	126
GO-PE (vdW only)	-	-	-	-	-	-	-	-	3.32	83

^a G_0 is taken as 4.0 nJ/m, the average of 3.4 and 4.6 nJ/m (for hydroxyl- and epoxide-rich GO, respectively. Values are calculated based on reference S4 and reference S5).

S4. Single-chain pull-off simulations for all polymers

Representative pulling force (F)-displacement (d), normalized force (F/N) and normalized number of hydrogen bonds (N_{HB}/N) curves for all polymers are shown in Fig. S4.

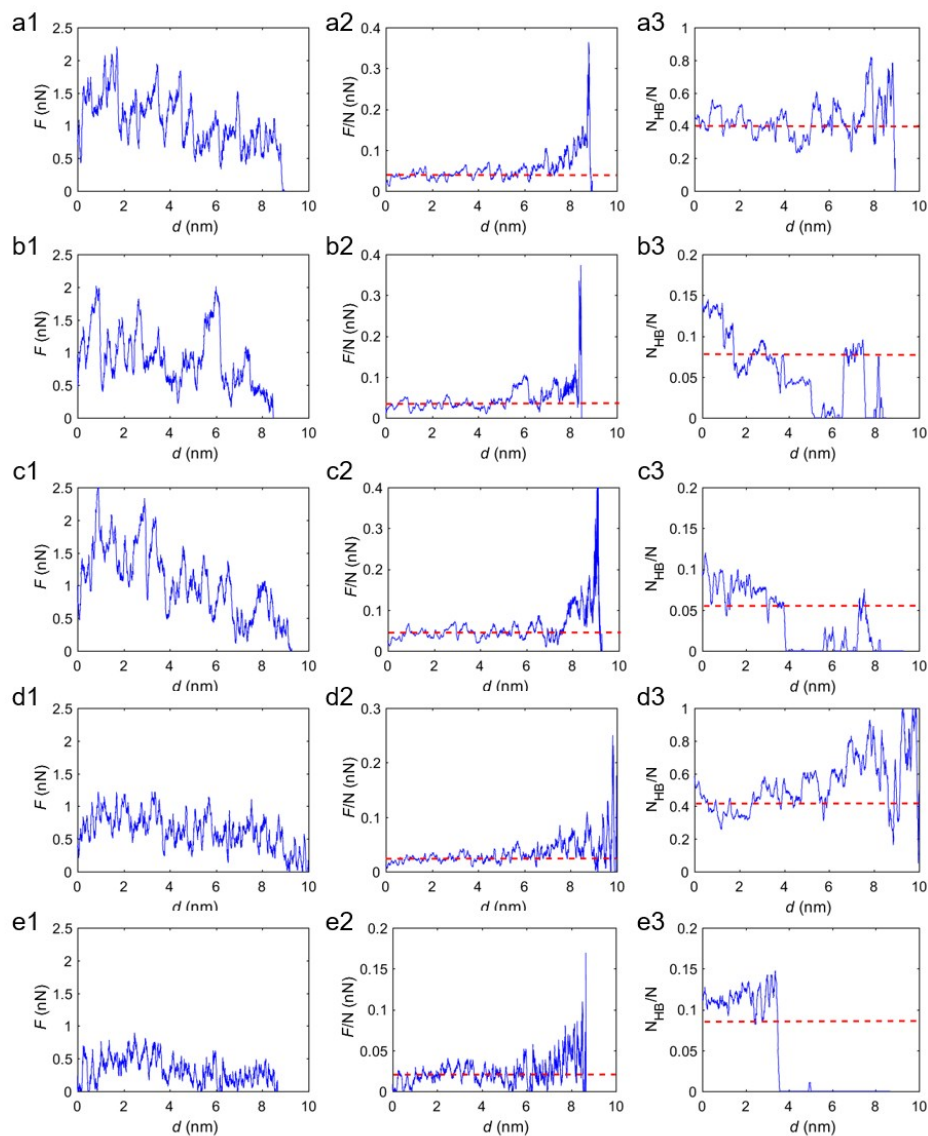


Fig. S4. Single-chain pull-off simulations for various polymers. The letter a-e represent curves for PAA, PMA, PBA, PVA and PEG, respectively. The numeral 1-3 represent F , F/N and N_{HB}/N for each polymer, respectively.

S5. Analysis of the cooperative behavior of HBs

To quantify the collective effects of HBs, we calculated the number of HBs that break in one stick-slip event. We looked at the difference between the force drops in such events in two types of single-chain pulling scenarios: shearing and peeling. Based on the method reported by Keten and Buehler,^{S6} we calculated and averaged $\Delta F_{peeling}$ and ΔF_{shear} for each polymer, as shown in Fig. S5. Then, the number of monomers involved in one stick-slip event was approximated by $N_{cr} = \Delta F_{shear} / \Delta F_{peeling}$. Notably, four HBs are cleaved at the GO-polymer interface in one stick-slip motion for PAA, compared with 3 for PVA. For the remaining three polymers, the values should be referred more accurately as ‘the number of clusters’ due to the more dominant contribution from van der Waals interactions.

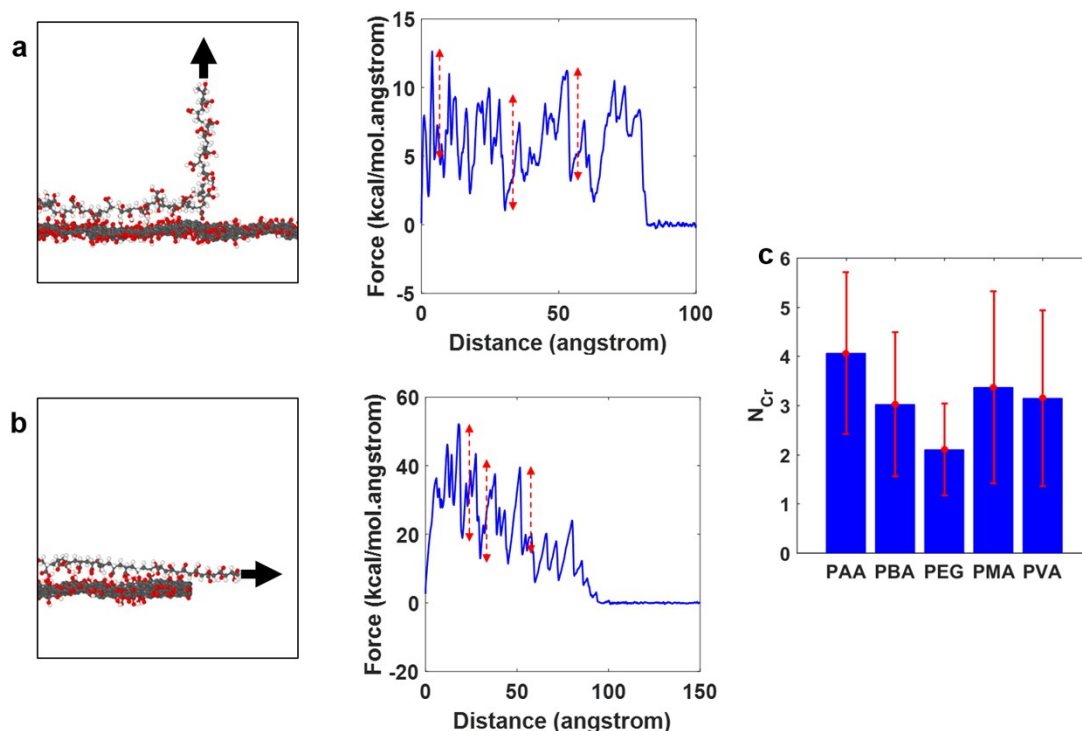


Fig. S5. Shear and peeling simulations to quantify the collective effect of HBs. (a) Peeling test of a single chain and its corresponding force-displacement curve. (b) Shearing test of a single chain and its corresponding force-displacement curve. In (a) and (b), $\Delta F_{peeling}$ and ΔF_{shear} are shown as the red dashed lines. (c) Average number of HBs (N_{cr}) that are cleaved in one stick-slip event, calculated as $\Delta F_{shear} / \Delta F_{peeling}$.

S6. Cost of computational resource

The use of the computational resource for the crack-opening simulations is shown in Table S3. A total amount of 80640 core hours were consumed. We also used ~ 40000 core hours to optimize the parameters and procedures for the simulations. The sum of the above two number, is \sim the total core hours we were assigned for this project. As a result, the number of simulations for each GO-polymer system was restricted to be 6. Nevertheless, with the aid of Student’s t-test to compare the average crack-bridging effect of different GO-polymer systems, we can still

compare the toughening performance of our selected set of polymers at an acceptable level of confidence. Together with the single-chain pull-off simulations, we successfully identified both chemical and geometrical effects that govern the extrinsic toughening of hydrogen-bonding-capable polymers on monolayer GO.

Table S3. Cost of computational resource for the crack-opening simulations

Polymer	Computation time per simulation (hour)	Number of simulations	Number of cores	Computation resource used (core hours)
PAA	40	6	64	15360
PMA	50	6	64	19200
PBA	60	6	64	23040
PVA	30	6	64	11520
PEG	30	6	64	11520

S7. Reference

- S1. M. Rubinstein and R. H. Colby, *Polymer physics*, Oxford University Press, New York, 2003.
- S2. Characteristic Ratio of Some Polymers, <http://polymerdatabase.com/polymer%20physics/C%20Table2%20.html>, (accessed January 05, 2018, 2018).
- S3. G. Bao and Z. Suo, *Appl. Mech. Rev.*, 1992, **45**, 355-366.
- S4. Z. X. Meng, R. A. Soler-Crespo, W. J. Xia, W. Gao, L. Ruiz, H. D. Espinosa and S. Keten, *Carbon*, 2017, **117**, 476-487.
- S5. I. Benedetti, H. Nguyen, R. A. Soler-Crespo, W. Gao, L. Mao, A. Ghasemi, J. Wen, S. Nguyen and H. D. Espinosa, *J. Mech. Phys. Solids*, 2018, **112**, 66-88.
- S6. S. Keten and M. J. Buehler, *Nano Lett.*, 2008, **8**, 743-748.